Chemical Physics Letters 884 (2026) 142558

Contents lists available at ScienceDirect

Chemical Physics Letters

journal homepage: www.elsevier.com/locate/cplett

Research paper

Formation of radical cations of *para*-substituted polystyrenes in dichloroethane by electron beam pulse irradiation

Kazumasa Okamoto [a,b,*], Yusa Muroya [a], Takahiro Kozawa [a]

[a] SANKEN (The Institute of Scientific and Industrial Research), The University of Osaka, Ibaraki, Osaka, 567-0047, Japan
[b] Artificial Intelligence Research Center, SANKEN (AIRC-SANKEN), The University of Osaka, Ibaraki, Osaka, 567-0047, Japan

ARTICLE INFO

Keywords:
Polystyrene
Poly(4-methoxystyrene)
Radical cation
Pulse radiolysis
Quantum chemical calculation

Transient absorption measurements were conducted on *para*-substituted polystyrene (PS) derivative radical cations formed in 1,2-dichloroethane using pulse radiolysis. While most PS radical cations are neutralized within microseconds, the poly(4-methoxystyrene) (PMOS) radical cation has a remarkably extended lifetime ($t_{1/2}$ = 680 μs), which is three orders of magnitude longer than that of PS. This stability is attributed to the formation of stable counterion pairs between the multimer radical cation (where holes are delocalized across multiple phenyl groups) and the Cl^- ions. Furthermore, the impact of substituent size on the formation of multimer radical cations in these PS derivatives was examined.

1. Introduction

Elucidation of the dynamics of radical cation species (one-electron oxidation) in polystyrene (PS) is becoming increasingly important for applications such as new electron beam (EB) and extreme ultraviolet (EUV) resist materials used in the lithography process [1–5], as well as for understanding the oxidative decomposition process in recycling [6–9]. When molecules are exposed to ionizing radiation, such as EB, their orbital electrons are knocked out, causing forced one-electron oxidation and the formation of radical cations [10]. Owing to its positive charge, a radical cation generally has a short lifetime because it readily combines with electrons or anions through Coulombic interactions.

The initial radiation-chemical process of PS derivatives has been investigated using EB pulse radiolysis [11–14], a time-resolved spectroscopic technique that uses an EB pulse as a pumping source [15–17]. In the solid phase, radical cations are predominantly formed through direct ionization. However, in the context of pulse radiolysis of PS solutions, the utilization of chlorinated solvents is frequently observed as a prevalent method for generating radical cations derived from solute molecules. For instance, when 1,2-dichloroethane (DCE) is used as the PS solvent (Fig. 1(a)), it is predominantly ionized, resulting in the formation of a DCE radical cation. This radical cation then initiates radiation-chemical reactions, as shown in Fig. 1(b). The DCE radical cations act as oxidants, reacting with solutes that have lower ionization potentials via hole transfer or one-electron oxidation. This process results in the transient formation of radical cations. [18–22]. The radical cation of a PS monomer unit undergoes an ion-molecule reaction with a neutral unit, resulting in the formation of an intramolecular dimer or multimer radical cation. The dimer radical cation is generated through a charge resonance (CR) interaction process, and the hole is delocalized between two adjacent phenyl rings (Fig. 1(c)) [12,13,23]. Another radiation-induced product in PS is an intramolecular excimer, which is formed by the interaction of a singlet excited state with a ground-state phenyl group. However, these rarely form in solutions with high concentrations of chlorinated hydrocarbons [11,24] because chlorinated hydrocarbons act as electron scavengers, that inhibit the formation of excited states. Studying reaction systems using DCE as a solvent is an effective way to elucidate the reaction mechanism and molecular dynamics of polymer radical cation species in chemically amplified resists

* Corresponding author at: SANKEN (The Institute of Scientific and Industrial Research), The University of Osaka, Ibaraki, Osaka 567-0047, Japan.
E-mail address: kazu@sanken.osaka-u.ac.jp (K. Okamoto).

https://doi.org/10.1016/j.cplett.2025.142558
Received 7 October 2025; Received in revised form 12 November 2025; Accepted 24 November 2025
Available online 25 November 2025

for semiconductor device fabrication. This is because chemically amplified resists contain high concentrations of photoacid generators that can trap electrons [1,10], and their compositions are similar to those of chemically amplified resists. However, research on the substituent dependence of the dynamics of radical cation species in PS is limited, despite its essential role in developing excellent resist polymers.

The reaction of radiation-induced products of chlorinated hydrocarbons, such as Cl^- and Cl atoms, with PS radical cations or neutral PS results in the formation of charge transfer (CT) complexes between the phenyl rings of PS and chlorine atoms [11,12]. The neutralization of the geminate ion pair (a radical cation and its corresponding anion or electron) formed after ionization typically occurs at a diffusion-controlled rate on a picosecond to nanosecond timescale, a process known as geminate ion recombination [25,26]. Conversely, bulk recombination between free ions is a considerably slower process that occurs over the order of milliseconds. These recombination processes compete with radical cation-mediated reactions, such as deprotonation and electron transfer to other solutes [27]. Consequently, the formation of stable ion pairs, which prevents the neutralization of positive and negative ions, is imperative for enhancing the efficiency and controllability of chemical reactions that utilize radical cations as intermediates [28–32].

In this study, we employed EB pulse radiolysis to generate radical cations of PS derivatives in DCE, thereby elucidating the substituent dependence at the *para* position of the phenyl ring. The results demonstrate that the radical cation of poly(4-methoxystyrene) (PMOS) remains stable for sub-millisecond timescales. A discussion was held regarding the factors that contribute to the long lifetime of the PMOS radical cation, focusing on quantum chemical calculations. Furthermore, the size effects of the substituents were also investigated.

2. Experimental and calculations

2.1. Pulse radiolysis measurements

In the pulse radiolysis method, we measured the photoabsorption of short-lived intermediates produced by irradiating polystyrene derivative solutions with EB pulses. The samples were argon-saturated solutions of PS derivatives in DCE (Sigma-Aldrich). We irradiated an optical cell containing the liquid sample with a synchronized EB pulse and analyzed the light from a xenon flash lamp. The kinetic traces had a time resolution of approximately 10 ns and wavelength range of 300–1600 nm. The EB pulses (26 MeV, 8 ns) used for irradiation were generated by the L-band LINAC at SANKEN, The University of Osaka.

2.2. Sample polymers

Polystyrene and *p*-substituted polystyrenes (Substituents = X)

1. Polystyrene (PS, X = H) Sigma-Aldrich, Mw = 13,200, Mn = 12,400
2. Poly(4-methylstyrene) (PMS, X = CH_3) Polymer Source, Mw = 42,900, Mn = 40,500
3. Poly(4-*tert*-butylstyrene) (PBS, X = *t*-Bu (*tert*-C_4H_9) Polymer Source, Mw = 41,800, Mn = 40,600
4. Poly(4-iodostyrene) (PIS, X = I) Scientific Polymer, Mw = 400,000
5. Poly(4-bromostyrene) (PBrS, X = Br) Polymer Source, Mw = 15,500, Mn = 13,000
6. Poly(4-chlorostyrene) (PClS, X = Cl) Polymer Source, Mw =25,500, Mn = 15,000
7. Poly(4-acetoxystyrene)(PAS, X = acetoxy (AC: $OCOCH_3$)) Polymer Source, Mw = 32,500, Mn = 18,000
8. Poly(4-methoxystyrene) (PMOS, X = OCH_3) Polymer Source, Mw = 19,500, Mn = 18,000
9. Poly(4-[*tert*-butoxycarbonyl]oxy-styrene (PTBOCS, X = *t*-BOCO (OCOO-*tert*-C_4H_9)) Polymer Source, Mw = 12,700 Mn = 11,300

2.3. Density functional theory (DFT) calculations

We used density functional theory (DFT) at the ωB97X-D/def2-TZVP level to calculate the optimized conformations of the radical cations for a portion of each polymer chain. For some calculations, the polarizable continuum model (PCM) was used to incorporate the solvent effects.

Ethylbenzene and isotactic (*m*) 2,4-diphenyl pentane derivatives were evaluated as monomer (monad) and dimer (diad) models, respectively. The ionization energies for these models were calculated from the difference in the standard Gibbs energies of formation between the radical cations and neutral molecules after structural optimization. We also performed time-dependent DFT (TD-DFT) calculations for the radical cation species. All DFT calculations were performed using the Gaussian16 Rev. C program [33], and the molecular structures were

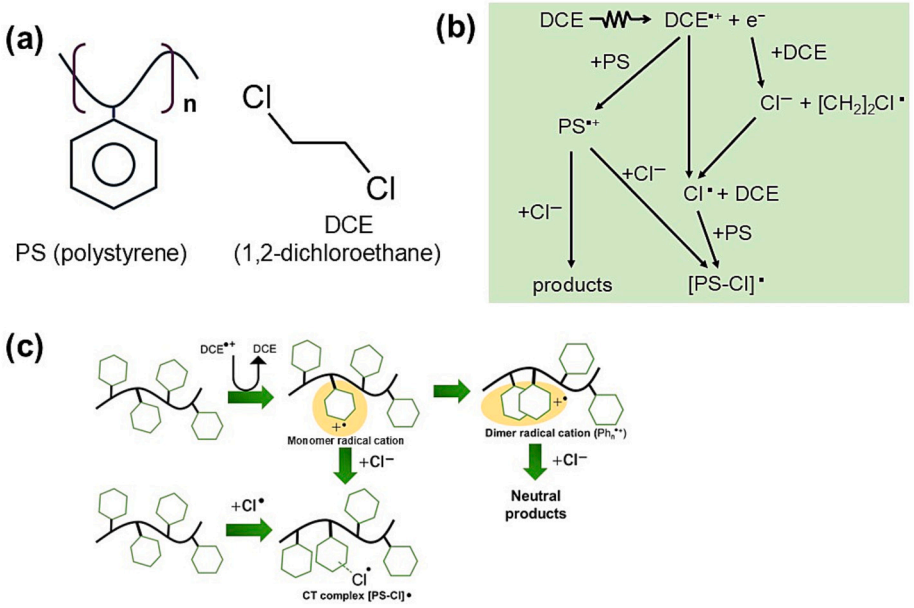

Fig. 1. Chemical structures of polystyrene (PS) and 1,2-dichloroethane (DCE). (b) Representative radiation-induced initial processes of PS in DCE. (c) The formation of monomer and dimer radical cations in the PS chain, as well as CT complex formation between the Cl atom and PS in DCE, is induced by radiation.

visualized using the Winmostar software [34].

3. Results and discussion

The pulse radiolysis method has been demonstrated to reveal the rapid dynamics of radiation-induced intermediates, primarily by monitoring the transient absorption and emission after EB irradiation. Furthermore, the identification of transient species is facilitated by the analysis of a combination of transient absorption and emission spectra. In this study, pulse radiolysis measurements of PS derivatives in Ar-saturated DCE were performed. The initial radiation-induced process of PS solution in DCE begins with solvent ionization, as shown in Fig. 1 (b). Electron attachment to DCE and electron transfer reactions between polystyrene (PS) and the DCE radical cation, as well as the formation of a CT complex between PS and Cl, occur in pseudo-first-order reactions when the concentrations of PS and DCE are sufficiently high and within the EB pulse irradiation time (< 8 ns). Geminate ion recombination (cation–anion/ electron pairs) typically occurs in less than a nanosecond, but is delayed by electron substitution onto Cl^-. This allows PS radical cation decay to be observed in the hundreds of nanosecond time domain [12]. Additionally, recombination reactions between free ions escaping from geminate ions (bulk recombination) occur within the microsecond time domain or longer. Additionally, dimer radical cation formation after hole transfer into PS predominantly occurs within the picosecond time domain [14]. Therefore, the primary reactions observed in the system studied via nanosecond pulse radiolysis are the decay of radical cations or CT complexes, though this may vary depending on the presence of substituents.

As illustrated in Fig. 2, the transient absorption spectra of PS (**A**) and PMOS (**B**) were recorded after EB pulse irradiation, accompanied by kinetic traces of the CR bands of the radical cation species in the near-infrared (NIR) region. As shown in Fig. 2(A), the transient absorption spectra of the PS solution were analogous to those previously reported in chlorinated solvents, including carbon tetrachloride, chloroform, and methylene chloride [12].The absorption bands around 500 nm were identified as CT complexes between phenyl rings and Cl atoms or ion pairs between phenyl radical cations and Cl^- [11,12]. Fig. 2(B) shows the transient absorption spectra obtained from the pulse radiolysis of the PMOS solution. Although the measurement wavelength for the PMOS kinetic trace was approximately 300 nm shorter than its absorption maximum (~1400 nm), the measurement was conducted at the strongest wavelength of the analyzing light source to ensure a long measurement time range and sufficient intensity. The identification of the absorption bands of PMOS solutions has been previously reported [13].

The PMOS solution exhibited a pronounced absorption band with a maximum at 480 nm. Although this peak wavelength is nearly identical to that observed in the PS solution, it corresponds to the local excitation (LE) band of the PMOS dimer cation. Furthermore, the absorption band at 1400 nm corresponds to the CR band of a dimer radical cation [35,36], which is also observed in PS [12,23,24]. However, the lifetimes of the CR band absorption differ significantly between PS and PMOS, with the PMOS value being more than three orders of magnitude longer (400 ns and 680 μs). The decay of the CR band for the PS dimer radical cation is assumed to occur via a diffusion-controlled process involving ion recombination between ion species, such as geminate ion recombination or bulk recombination. This behavior arises from diffusion reactions under a Coulomb field due to reactions between ion species and is therefore distinct from a first-order reaction [25]. Furthermore, the absorption intensity of PMOS is more than twice that of PS. This observation suggests the presence of long-lived PMOS radical cation species in this system. **Fig. S1** in the Supplementary Information provides details of the transient absorption spectra and time profiles of the other derivatives. All the derivatives shown here typically exhibit a CR band in the NIR region due to the dimer radical cation. The measured lifetimes and absorption maxima of the CR band are summarized in Table 1. In a manner consistent with other PS derivatives, those with electron-withdrawing substituents (I, Br, and Cl) exhibited lifetimes nearly equivalent to those of PS (several hundred nanoseconds). The acetoxy group (AC) has been previously reported to have a Hammett constant (σ_p) of 0.31 at the *para* position [37], indicating very strong electron-withdrawing properties. However, a recent reevaluation identified a slight electron-donating tendency, as evidenced by a σ_p of −0.02 [38]. The CR band absorption lifetime of poly(4-acetoxystyrene) (PAS)

Table 1
The maximum (λ_{MAX}) and lifetime of CR band absorption of PS and its derivatives radical cations, as obtained by the pulse radiolysis method.

Polymers	Substituents	λ_{MAX} (CR band) [nm]	Lifetime [s]
PS	H	1250	4.0×10^{-7}
PMS	CH_3	1300	6.0×10^{-6}
PBS	*t*-butyl (*t*-Bu)	1250	6.3×10^{-7}
PIS	I	1500	2.8×10^{-7}
PBrS	Br	1450	3.3×10^{-7}
PClS	Cl	1450	2.9×10^{-7}
PAS	Acetoxy (AC)	1200	1.6×10^{-6}
PMOS	OCH_3	1400	6.8×10^{-4}*
PTBOCS	*t*-BOCO	1150	1.4×10^{-6}

* Kinetics analysis was performed at 1100 nm.

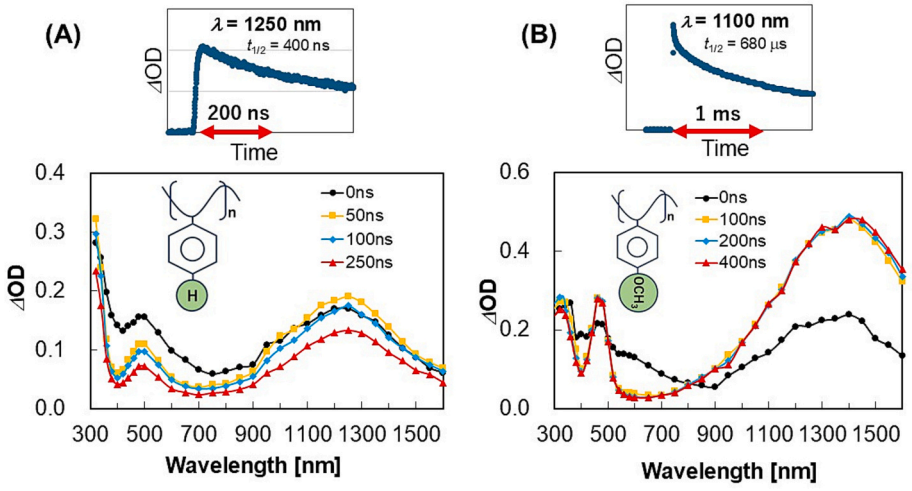

Fig. 2. The transient absorption spectra of Ar-saturated 100 mM (unit conc.) PS solutions (A) and PMOS solutions (B) in DCA were obtained by EB pulse radiolysis at 0, 50, 100, and 250 ns after 8 ns of EB irradiation. The kinetic traces of the CR bands at 1250 nm (A) and 1100 nm (B) are shown in the figure.

was 1600 ns, which is more than twice as long as that of PS or PS derivatives with electron-withdrawing groups. Furthermore, a discrete absorption band was observed at 600 nm. The identification of this band was inferred from the decrease in the absorption intensity accompanying the increase in the CR band absorption of the dimer radical cation. Its wavelength is distinct from those of both the polystyrene-Cl charge-transfer (CT) complex and local excitation (LE) bands, suggesting that it is due to the absorption by the free monomer radical cations of the PS derivatives (Fig. 1(c)). In addition, comparable absorption bands around 600 nm have been observed in other polyoxystyrenes, including PAS, poly(4-[*tert*-butoxycarbonyl]oxy-styrene) (PTBOCS) and poly(4-methylstyrene) (PMS). This behavior, which corresponds to the absorption of free monomer radical cations, suggests that the structural relaxation process for the formation of dimer radical cations in polyoxystyrenes and PMS may involve a relatively slow mode occurring on a timescale of several tens of nanoseconds (**Fig. S2**), in addition to the fast formation modes that occur on a timescale of picoseconds to nanoseconds **[14]**. The equilibrium between monomer and dimer radical cations is strongly shifted toward the dimer due to stabilization by hole delocalization, and monomer radical cations rapidly form dimer radical cations **[35]**. Furthermore, Tojo et al. reported observing the absorption peak wavelength of the monomer compound (4-methoxystyrene) radical cation at 600 nm in DCE **[39]**, which supports this identification.

In addition, the poly(4-iodostyrene) (PIS) solution exhibited a more gradual pattern of absorption bands than the other solutions (**Fig. S1D**). This phenomenon is likely attributable to its elevated molecular weight (Mw = 400,000), which may significantly influence the intramolecular interactions. The findings indicate that PMOS exhibits an exceptionally long lifetime. Furthermore, the PMS sample demonstrated a relatively extended lifetime of 5.98 μs, suggesting that the electron-donating properties of the substituents play a significant role in prolonging the lifetime of the radical cation. However, the poly(4-*tert*-butylstyrene) (PBS) sample exhibited a lifetime of only 630 ns. Notwithstanding its Hammett constant ($\sigma_p = -0.2$), which is marginally more electron-donating than that of methyl ($\sigma_p = -0.17$) **[35]**, the lifetime of PBS is not considerably longer than that of PS (400 ns).

The diffusion-controlled reaction rate of bulk recombination between free ion pairs is estimated as follows:

$$k = 4\pi D r_c \tag{1}$$

where k is the reaction rate constant, D is the diffusion coefficient (cm^2s^{-1}), and r_c is the Onsager distance (Eq. (2)) **[40]**,

$$r_c = \frac{e^2}{\epsilon k_B T} \tag{2}$$

In this equation, e, ϵ, kB, and T represent the elementary charge (1.602×10^{-19}C), the dielectric constant ($10.37 \times \epsilon$, where $\epsilon = 8.854 \times 10^{-12}$ fm^{-1}), Boltzmann's constant (1.38×10^{-23} JK^{-1}), and temperature, respectively. It was hypothesized that r_c is sufficiently larger than the radius of the ion species. Employing this equation, r_c in DCE at 298 K was calculated to be 7.2 nm. The initial free ion concentration after EB irradiation was calculated to be 2.4×10^{-5} M based on the irradiation dose (270 Gy), free ion yield in DCE (G-value = 0.68/100 eV **[41]**), and DCE density (1.25 gcm^{-3}, 298 K). The mobility of 1×10^{-5} cm^2s^{-1} for Cl^- in DCM **[25]** was employed to predict the reaction rate constant, k, to be 5.5×10^{10} M^{-1} s^{-1}, which corresponds to a half-life of approximately 760 ns. It is also noteworthy that the diffusion coefficient of Cl^- in DCE is presumably lower than that in DCM because DCE exhibits slightly higher polarity and viscosity. Consequently, the calculated half-life in DCE was slightly prolonged. This aligns with the observations reported by Yamamoto et al. **[42]**, who noted that the reaction rate constant between the biphenyl radical cation and Cl^- was 1.5 times higher in DCM than in DCE. Consequently, the bulk recombination lifetime was calibrated to approximately 1.1 μs. A comparison of the lifetimes of the PS dimer radical cations, as determined by pulse radiolysis, exhibited strong agreement with this prediction, except for PMOS and PMS. The half-lives of these dimer radical cations ranged from several hundred nanoseconds to 1.6 μs (Table 1). These values are slightly faster than or comparable to those predicted for bulk recombination alone, suggesting that delayed geminate ion recombination plays a role, particularly for radical cations with shorter half-lives. This indicates that the dimer radical cations undergo diffusion-controlled recombination with Cl^-. However, PMOS and PMS are considered reaction-limited, as evidenced by their long lifetimes.

To elucidate the remarkably prolonged lifetime of the PMOS radical cation, a series of quantum chemical calculations were conducted. These calculations evaluated a model in which holes were localized within an isolated PS derivative polymer in the diad (dimer model) and monad (monomer model) (Fig. 3(A)). We conducted geometry optimizations and vibrational frequency calculations for the radical cation and neutral states of the two distinct models. These calculations were performed under vacuum and in DCM, using the polarizable continuum model (PCM). With respect to the dimer model, two stereoregularities have been identified: *meso* (*m*) and *racemo* (*r*) (**Fig. S3**). The *m* exhibits a configuration in which the side chains along the main chain are aligned in the same direction (isotactic), whereas the *r* exhibits a structure in which the side chains are aligned in the opposite direction to the main chain (syndiotactic). Excluding mirror images and conformations with significant steric hindrance, the stable conformations can be statistically classified into three types for *m*-isomers and five types for *r*-isomers based on the dihedral angle of *gauche* (*g*±: ∓60∘) or *trans* (*t*: 180∘) relative to the main-chain carbon. In this study, the *m-tt* conformation was examined in depth as it pertains to the most stable dimer radical cation structure. For the radical cation of the *r*-isomer, the most stable structure is the *r-tg*$^+$ conformation, which is stabilized by CR interactions and features stacked phenyl rings. In contrast, previous studies have demonstrated that for neutral molecules, the most stable conformation for both *m*- and *r*-stereoregularities is the trans–trans (*tt*) conformation **[43]**.

The long-term stability of PMOS radical cations indicates a low probability of electron transfer reactions with Cl^-, as shown in Eq. (3),

$$PS^+ + Cl^- \rightleftharpoons PS + Cl \tag{3}$$

According to the Gibbs energy change approximation for electron transfer in solution **[44]**, a lower oxidation potential of the neutral PS donor molecule renders the reverse reaction in Eq. (3). It is more probable that this will extend the lifetime of radical cations. Given the established correlation between the oxidation potential and ionization energy, the ionization energies for the dimer and monomer models of each derivative were determined. These values were derived from the energy difference between the optimized radical cation and ground state of each model, as shown in Fig. 3(B). The comparison results are displayed for the ionization energies of the dimer and monomer in vacuum (a) and the dimer model in vacuum and DCE (b). The ionization energies of the monomer and dimer models with substituents were lower than those of the PS model owing to the resonance effects. Among these models, PMOS with a strong electron-donating group exhibited the lowest value. Conversely, the difference in ionization energy caused by the presence or absence of a solvent indicates a solvation effect. The solvation effects of the *tert*-butoxycarbonyl]oxy (*t*-BOCO), acetoxy (AC), and *t*-butyl (*t*-Bu) groups, which possess large substituent sizes, were estimated to be 15–27 % smaller than those of PS.

Furthermore, quantum chemical calculations were performed using the PCM for neutral monomer and dimer models, with Cl atoms positioned near the phenyl groups. This was done to investigate the charge separation behavior between the Cl atom and the monomer/dimer sites during ion-pair contact (**Fig. S4**). The results demonstrated that the estimated charge separation was approximately 0.4 for both the dimer (PS2-Cl) and monomer (PS-Cl) models in the PS, indicating a dominant CT complex character. Based on the properties of benzene-chlorine atom

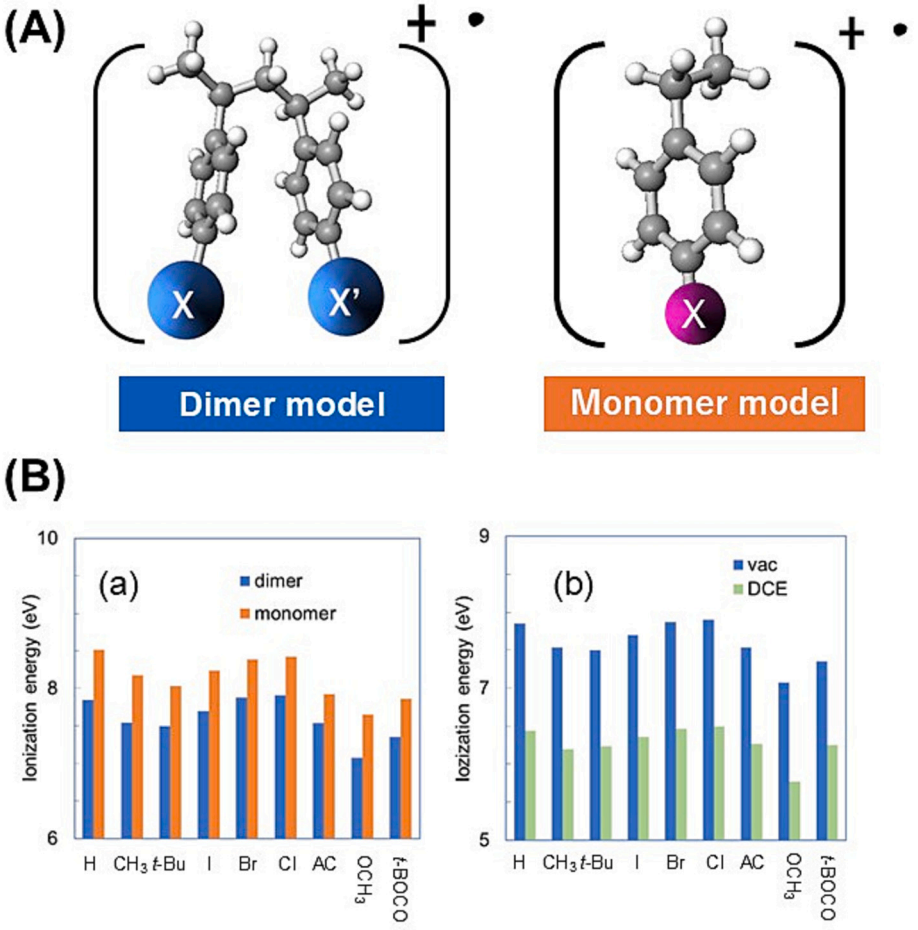

Fig. 3. Analysis of the radical cation models of PS and *p*-substituted PS derivatives. Dimer and monomer structure models of radical cations evaluated by DFT calculations (*para-substituted m* − 2,4-diphenylpentane and *para-substituted* ethylbenzene). (B) Ionization energies (IEs), obtained via DFT calculations, are the differences between the standard Gibbs energies of the structure-optimized radical cations and the neutral molecules. Each shows the substituents of the phenyl groups of the monomer and dimer models. (a) IEs of dimer and monomer models in vacuum. (b) IEs of dimer models in vacuum and DCE.

CT complexes [45], it is plausible to assume that PS derivatives also form CT complexes involving the π and/or σ electrons of the phenyl ring and the Cl atom. Crucially, the formation of this type of CT complex induces hydrogen abstraction reactions by the chlorine atom [46,47].

However, for the PMOS dimer (PMOS2-Cl) and monomer (PMOS-Cl) models, the estimated values were 0.82 and 0.65, respectively. These findings demonstrate that the substituent and CR effects enhance the ionic character of PMOS2-Cl. Furthermore, time-dependent (TD)-DFT calculations on PMOS2-Cl revealed a CR band in the NIR region for PMOS-Cl ($\lambda = 958.84$ nm, $f = 0.0711$). In contrast, the PS-Cl model ($\lambda =$ 939.61 nm, $f = 0.0004$) exhibited negligible oscillator strength. In the DCE system (Fig. 1(b)), the generation of Cl atoms was attributed to DCE radiolysis. In contrast to other PS derivatives, this observation indicates that PMOS possesses a distinctive capacity to form an ion pair, specifically a PMOS radical cation and Cl^-, through the reaction between a Cl atom and PMOS, as demonstrated by the reverse reaction in Eq. (3). As illustrated in Fig. 2, the absorption intensity of the PMOS CR band exceeded that of PS and its other derivatives by more than twofold. However, TD-DFT calculations of the dimer model revealed no significant difference in the oscillator strength (or absorption coefficient) between the PS and PMOS dimer radical cations. This suggests that PMOS produces a higher concentration of dimer radical cations than PS, which supports the significant contribution of the reverse reaction of Eq. (3). The formation of the PS^+–Cl^- ion pair is primarily driven by positive–negative Coulomb interactions. Following the formation of the counterion pair, the electron-donating substituents of CH_3O or CH_3 increase the π electron density of the phenyl groups. Consequently, one-electron reduction of the radical cation becomes less likely. This reduces the driving force for electron transfer from Cl^- to PS^+, thereby slowing the reaction rate. Consequently, the lifetime of PS^+ bearing electron-donating substituents is expected to increase. It has been determined that the lifetime of the long-lived PMOS radical cation is influenced by electron transfer between the radical cation and Cl^-, as well as by deprotonation reactions from the radical cation [48].

Given that the dimer model exhibits a considerably lower degree of polymerization than the authentic polymer, its influence was also examined. The wavelength of the CR band correlates with the extent of hole delocalization across phenyl units. It has been demonstrated that greater spreading leads to red shift [35,49]. Therefore, a comparative analysis was conducted between the pulse radiolysis results and the TD-DFT-calculated CR band wavelengths. As shown in Fig. 4, and **Table S1**, a comparison was made between the transient absorption spectra (pulse radiolysis) and the calculated CR band absorption (TD-DFT in a vacuum). While the experimentally determined wavelengths were longer than the TD-DFT predictions for derivatives with smaller substituents, good agreement was observed for derivatives with relatively larger substituents (*t*-Bu, AC, and *t*-BOC).

Furthermore, PCM model calculations that incorporated the solvent effect (DCE) revealed that derivatives with smaller substituents exhibited longer wavelength shifts than those in the vacuum (**Fig. S5 and Table S1**). This phenomenon is hypothesized to be due to a decline in CR interactions, which is a consequence of solvent polarity. DFT

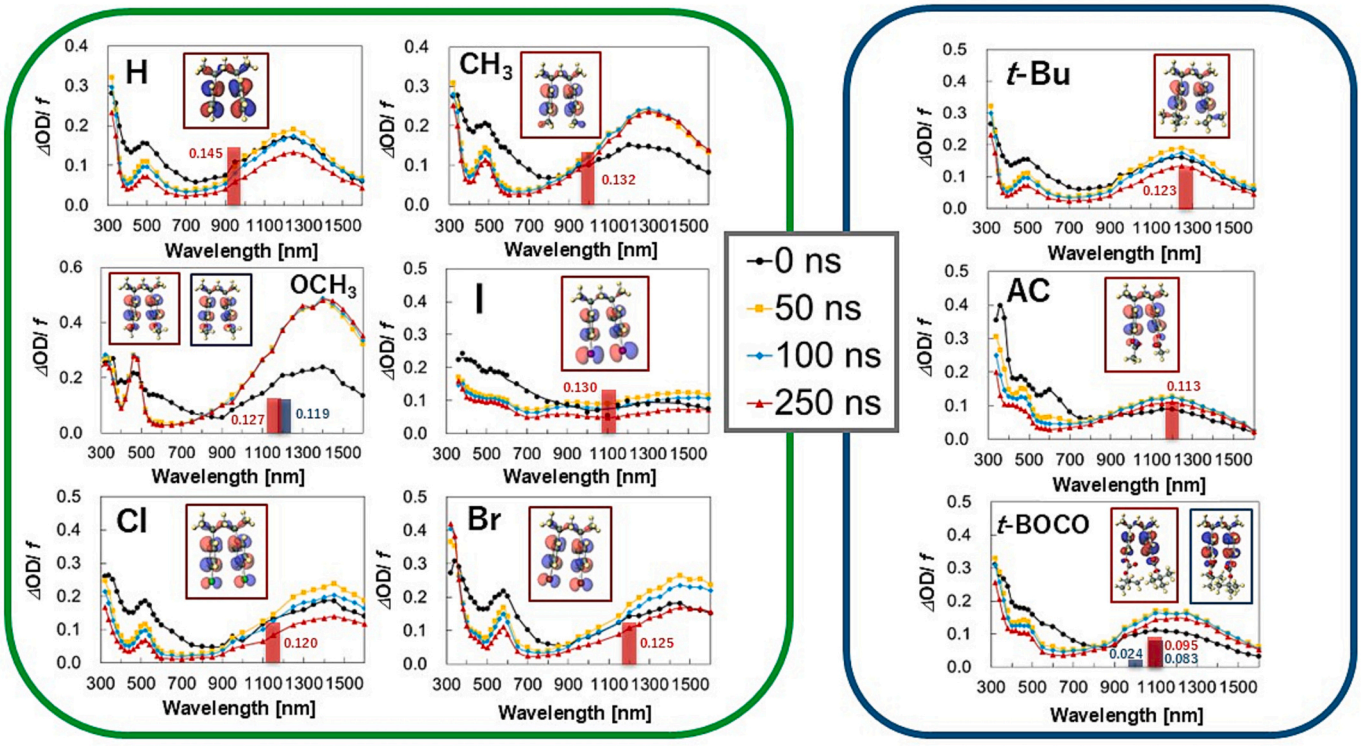

Fig. 4. Transient absorption spectra obtained at 0, 50, 100, and 250 ns after irradiation of Ar-saturated 100 mM (unit. Conc.) PS and its *p*-substituted derivatives in DCE solutions with an 8 ns electron beam (EB) pulse using nanosecond pulse radiolysis. The phenyl group substituents are indicated in the spectra. The spectra on the left (green box) show the small substituent groups, and the spectra on the right (blue box) show the large substituent group. The LUMO electronic states of the optimized dimer model structures obtained via DFT calculations, as well as the CR band wavelengths and oscillator strengths of the dimer models obtained via TD-DFT calculations are also shown in the spectra. Each number indicates an oscillator strength. PS derivatives substituted with OCH_3 and *t*-BOCO groups had two stable conformations that depended on the orientation of the substituents. OCH_3: (opposite orientation (*anti*-conformation, red) and same orientation (*syn*-conformation, blue). *t*-BOCO: (*syn*-conformation, red) and (*anti*-conformation, blue). The box colors of the dimer models correspond to the bar colors of the CR bands obtained using TD-DFT. (For interpretation of the references to colour in this figure legend, the reader is referred to the web version of this article.)

calculations in DCE showed that the optimized dimer structures had shorter distances between the phenyl rings than those in the vacuum condition (**Table S2**). This finding suggests that solvent effects stabilize structures with smaller molecular sizes.

Next, we considered derivatives with larger substituents, such as *t*-Bu, AC, and *t*-BOC. With the addition of the solvent effect, the CR band of *t*-Bu shifted to a longer wavelength, and the distance between the phenyl rings increased (**Table S2**), similar to that observed for smaller substituent groups. Conversely, for AC and *t*-BOC, which contain highly polar carbonyl groups, the calculation results incorporating the solvent effect showed a greater distance between the phenyl rings in the dimer models. This suggests that the solvation effect on the substituents is stronger than that on the phenyl rings. Furthermore, when considering the solvent effect, the CR band of the *anti*-conformation of the dimer model with *t*-BOC, in which the holes were almost equally delocalized between the phenyl groups, was red-shifted (shifted to longer wavelengths). This result is consistent with those observed for other derivatives. However, in some cases, such as for AC and *t*-BOC (*syn*-conformation), the CR characteristics were weakened owing to the hole localization at one of the phenyl groups of the dimer. This resulted in a blue shift in the NIR transition.

Notably, dimer model does not fully represent a real polymer because it does not include units adjacent to the dimer. Consequently, the solvent effect was inherently emphasized in the dimer model. Therefore, when comparing the predicted CR band absorption wavelengths with the pulse radiolysis results, the intermediate trend between the vacuum and DCE results should be considered. Under this consideration, the TD-DFT calculations indicate that, for the dimer model with small substituents, the CR band wavelength is shorter than the experimental value. This suggests that the holes were delocalized beyond the dimers. Conversely, derivatives with large substituents have CR band wavelengths that are relatively close to those of the delocalized-holes dimer model. Therefore, the holes can be considered to be contained mainly within dimers. This is likely because steric hindrance prevents the effective stacking of multiple phenyl groups, thereby keeping most holes confined within the dimer unit.

The long-lived properties of PMOS radical cations are believed to be attributable to the reduction in ionization energy across multiple monomer units within the polymer. This ionization energy reduction can be attributed to two key factors: the electronic substituent effect leading to a large CR within the polymer's phenyl groups, and a relatively smaller steric hindrance. The present study suggests that the strategic adjustment of the ionization energy by *para*-substituents in PS is crucial for controlling the reaction pathway of the generated radical cation. Specifically, the knowledge that lowering the ionization energy promotes the deprotonation pathway as the deactivation route for stabilized radical cations provides significant guidance in resist polymer design.

4. Conclusions

In this study, pulse radiolysis was performed on polystyrene (PS) derivatives in 1,2-dichloromethane (DCE). In addition, quantum chemical calculations were used to examine the impact of substituents on the dynamics of the locally formed radical cation species within the PS chain. These findings are expected to be useful for developing resist materials for nano/microfabrication that utilize condensed-phase ionization reactions, as well as for developing novel synthesis methods via

the formation of radical cation species.

The enhancement of the sensitivity of chemically amplified resist materials for the mass production of semiconductor devices is contingent upon the augmentation of the deprotonation efficiency of the radical cation species generated by ionizing radiation [10]. Hydroxyl and carbonyl groups are proton sources and proton-accepting groups, respectively, which are frequently incorporated into resists to facilitate deprotonation (acid generation) [50]. Furthermore, the incorporation of nonpolar groups, such as protected hydroxyl and polystyrene groups, regulates the solubility of the resist during the development process, converting the latent image into a visible image. In this study, we demonstrated that PS-based molecules with small, strong electron-donating substituents, such as methoxy groups (PMOS), enhance the stability of radical cations. Despite the absence of acidic protons or carbonyl groups in PMOS, the proton yield of PMOS in solid thin films is approximately half that of PHS [48]. The findings of this study indicate that the PMOS radical cation demonstrates reduced susceptibility to neutralization reactions, such as electron transfer from Cl^-. Although the deprotonation reaction is relatively slow, the PMOS radical cation is expected to generate sufficient protons because of its extended sub-millisecond lifetime.

Moreover, recent advancements in photoredox catalysis have led to reports of chemical synthesis reactions involving stable methoxy-substituted radical cations [28–32]. The stability behavior of the PMOS radical cation observed in this study is consistent with these results. However, the limited lifetimes of these species significantly restrict their utilization in synthetic chemistry, even at low temperatures. Consequently, the insights derived from this study are anticipated to lay the foundation for novel synthetic methodologies.

CRediT authorship contribution statement

Kazumasa Okamoto: Writing – original draft, Methodology, Investigation, Funding acquisition, Conceptualization. **Yusa Muroya:** Writing – review & editing, Methodology. **Takahiro Kozawa:** Writing – review & editing, Resources, Funding acquisition.

Fundings

This work was partially supported by a Grant-in-Aid for Scientific Research (Project No. 25K08526, 22K04986, and 24H00443) from the Ministry of Education, Culture, Sports, Science and Technology, Japan (MEXT).

Declaration of competing interest

The authors declare the following financial interests/personal relationships which may be considered as potential competing interests: Kazumasa Okamoto reports financial support was provided by Ministry of Education, Culture, Sports, Science and Technology, Japan (MEXT). Takahiro Kozawa reports financial support was provided by Ministry of Education, Culture, Sports, Science and Technology, Japan (MEXT). If there are other authors, they declare that they have no known competing financial interests or personal relationships that could have appeared to influence the work reported in this paper.

Acknowledgements

The authors wish to express their gratitude to the members of the Research Laboratory for Quantum Beam Science, SANKEN, The University of Osaka, for performing the pulse radiolysis measurements.

Appendix A. Supplementary data

Supplementary data to this article can be found online at https://doi.org/10.1016/j.cplett.2025.142558.

Data availability

The authors confirm that the main data supporting the findings of this study are available within the article and its supplementary materials. Other data that supporting the findings of this study are available from the corresponding author [K. Okamoto], upon reasonable request.

References

[1] H. Ito, Chemical amplification resists for microlithography, in: Microlithography · Molecular Imprinting. Advances in Polymer Science 172, Springer, Berlin, Heidelberg, 2005, https://doi.org/10.1007/b97574. ISBN: 9783540218623.
[2] C.K. Ober, F. Käfer, C. Yuan, Recent Developments in Photoresists for Extreme-Ultraviolet Lithography, Polymer 280 (2023) 126020, https://doi.org/10.1016/j.polymer.2023.126020.
[3] Y. Zhang, H. Yu, L. Wang, X. Wu, J. He, W. Huang, C. Ouyang, et al., Advanced Lithography Materials: From Fundamentals to Applications, Adv. Colloid Interface Sci. 329 (2024) 103197, https://doi.org/10.1016/j.cis.2024.103197.
[4] T. Kozawa, Design Strategy of Extreme Ultraviolet Resists, Jpn. J. Appl. Phys. 63 (2024) 050101, https://doi.org/10.35848/1347-4065/ad3a4c.
[5] S. Ma, C. Con, M. Yavuz, B. Cui, Polystyrene Negative Resist for High-Resolution Electron Beam Lithography, Nanoscale Res. Lett. 6 (2011) 1–6, https://doi.org/10.1186/1556-276X-6-446.
[6] A. Ong, Z.C. Wong, K.L.O. Chin, W.W. Loh, M.H. Chua, S.J. Ang, J.Y.C. Lim, Enhancing the Photocatalytic Upcycling of Polystyrene to Benzoic Acid: A Combined Computational-Experimental Approach for Acridinium Catalyst Design, Chem. Sci. 15 (2023) 1061–1067, https://doi.org/10.1039/d3sc06388g.
[7] S. Jiang, Y. Chen, Y. Huang, P. Hu, Photooxidation of Polystyrene into High-Value Chemicals, Eur. J. Org. Chem. 202401109 (2024), https://doi.org/10.1002/ejoc.202401109.
[8] A.L. De Abreu, D. Taton, D.M. Bassani, Reassessing the Photochemical Upcycling of Polystyrene Using Acridinium Salts, Angew. Chem. Int. Ed. 202418680 (2024), https://doi.org/10.1002/anie.202418680.
[9] D. Baek, A.J. Al Abdulghani, D.J. Walsh, D.T. Hofsommer, J.B. Gerken, C. Shi, E.Y. X. Chen, et al., Can the hock process be used to produce phenol from polystyrene? J. Am. Chem. Soc. 147, 10 (2025) 8637–8694, https://doi.org/10.1021/jacs.4c18143.
[10] T. Kozawa, S. Tagawa, Radiation Chemistry in chemically amplified resists, Jpn. J. Appl. Phys. 49 (2010) 030001, https://doi.org/10.1143/JJAP.49.030001.
[11] M. Washio, S. Tagawa, Y. Tabata, Pulse radiolysis of polystyrene and benzene in cyclohexane, chloroform and carbon tetrachloride, Radiat. Phys. Chem. 21 (1983) 239–243, https://doi.org/10.1016/0146-5724(83)90152-8.
[12] K. Okamoto, T. Kozawa, Y. Yoshida, S. Tagawa, Study on Intermediate Species of Polystyrene by Using Pulse Radiolysis, Radiat. Phys. Chem. 60 (2001) 417–422, https://doi.org/10.1016/S0969-806X(01)00183-9.
[13] K. Okamoto, M. Tanaka, T. Kozawa, S. Tagawa, Dynamics of Radical cation of poly (4-Hydroxystyrene)-based chemically amplified resists for extreme-ultraviolet and Electron beam Lithographies, 2010, Jpn. J. Appl. Phys. 49 (2010) 106501, https://doi.org/10.1143/JJAP.49.106501.
[14] M. Gohdo, S. Tagawa, K. Kan, J. Yang, Y. Yoshida, Direct Ionization-Driven Observational Approaches for Radical Cation Formation in Solution for Pulse Radiolysis, Radiat. Phys. Chem. 196 (2022) 110105, https://doi.org/10.1016/j.radphyschem.2022.110105.
[15] Z. Jiang, C. Clavaguéra, S.A. Denisov, J. Ma, M. Mostafavi, Role of oxide-derived cu on the initial elementary reaction intermediate during catalytic CO_2 reduction, J. Am. Chem. Soc. 146, 44 (2024) 30164–30173, https://doi.org/10.1021/jacs.4c08603.
[16] Z. Jiang, M. Mostafavi, Direct observation of the reactivity of electrons toward gold nanoparticles in aqueous solution, Nano Lett. 24 (2024) 12249–12253, https://doi.org/10.1021/acs.nanolett.4c03396.
[17] K. Kobayashi, Pulse Radiolysis Studies for Mechanism in biochemical redox reactions, Chem. Rev. 119 (6) (2019) 4413–4462, https://doi.org/10.1021/acs.chemrev.8b00405.
[18] T. Sumiyoshi, N. Sugita, K. Watanabe, M. Katayama, Pulse Radiolysis Studies of Solvent Radical Cations in Liquid 1,2-Dichloroethane, Bull. Chem. Soc. Jpn. 61 (1988) 3055–3059, https://doi.org/10.1246/bcsj.61.3055.
[19] N.E. Shank, L.M. Dorfman, Pulse Radiolysis Studies, XVII., Reaction kinetics of molecular cations of aromatic compounds in dichloroethane solution, J. Chem. Phys. 52 (9) (1970) 4437–4440, https://doi.org/10.1063/1.1673670.
[20] A.M. Funston, J.R. Miller, Increased yields of Radical cations by Arene addition to irradiated 1,2-dichloroethane, Radiat. Phys. Chem. 72 (5) (2005) 601–611, https://doi.org/10.1016/j.radphyschem.2004.03.014.
[21] D.E. Polyansky, G.F. Manbeck, M.Z. Ertem, Combined effects of Hemicolligation and ion pairing on reduction potentials of biphenyl Radical cations, J. Phys. Chem. A 127 (38) (2023) 7918–7927, https://doi.org/10.1021/acs.jpca.3c03817.
[22] M. Yamaji, Y. Osakada, S. Tojo, M. Fujitsuka, Radiochromism of Spiropyran via the Radical Ions Studied by Pulsed Electron Radiolysis and DFT Calculation, Radiat. Phys. Chem. 227 (2025) 1–5, https://doi.org/10.1016/j.radphyschem.2024.112393.
[23] S. Irie, H. Horii, M. Irie, Radical Ions of Vinyl Polymers Having Aromatic Side Groups. Polystyrene and Poly(2-vinylnaphthalene), Macromolecules 13 (6) (1980) 1355, https://doi.org/10.1021/ma60078a006.

[24] K. Okamoto, T. Kozawa, M. Miki, Y. Yoshida, S. Tagawa, Pulse Radiolysis of polystyrene in cyclohexane - effect of carbon tetrachloride on kinetic dynamics of dimer Radical cation, Chem. Phys. Lett. 426 (4–6) (2006) 306–310, https://doi.org/10.1016/j.cplett.2006.05.115.
[25] K. Ushida, Y. Yoshida, T. Kozawa, S. Tagawa, A. Kira, Evidence of oxidation of aromatic hydrocarbons by chloromethyl radicals: reinvestigation of Intersolute hole transfer using pulse Radiolysis, J. Phys. Chem. A 103 (24) (1999) 4680–4689, https://doi.org/10.1021/jp9841900.
[26] A. Saeki, N. Yamamoto, Y. Yoshida, T. Kozawa, Geminate charge recombination in liquid alkane with concentrated CCl_4: effects of CCl_4 Radical anion and narrowing of initial distribution of cl^-, J. Phys. Chem. A 115 (36) (2011) 10166–10173, https://doi.org/10.1021/jp205989r.
[27] M. Schmittel, A. Burghart, Understanding Reactivity Patterns of Radical Cations, Angew. Chem. Int. Ed. 36 (1997) 2550–2589, https://doi.org/10.1002/anie.199725501.
[28] J.K. Kochi, R. Rathore, P. Le Maguéres, Stable dimeric aromatic cation-radicals. structural and spectral characterization of through-space charge delocalization, J. Org. Chem. 65 (21) (2000) 6826–6836, https://doi.org/10.1021/jo000570h.
[29] T.N. Komatsu, K. Komatsu, Persistent Radical, Cations: Self-Association And Its Steric Control in The Condensed Phase, Org. Biomol. Chem. 3 (2005) 561–569, https://doi.org/10.1039/b418872a.
[30] T. Shimajiri, S. Kawaguchi, T. Suzuki, Y. Ishigaki, Direct Evidence for a Carbon–Carbon One-Electron σ-bond, Nature 634 (2024) 347–352, https://doi.org/10.1038/s41586-024-07965-1.
[31] L. Guo, R. Chu, X. Hao, Y. Lei, H. Li, D. Ma, G. Wang, et al., Ag_3PO_4 enables the generation of long-lived Radical cations for visible light-driven [2+2] and [4+2] pericyclic reactions, Nat. Commun. 15 (1) (2024) 1–11, https://doi.org/10.1038/s41467-024-45217-y.
[32] T. Horibe, S. Ohmura, K. Ishihara, Structure and reactivity of aromatic Radical cations generated by $FeCl_3$, J. Am. Chem. Soc. 141 (5) (2019) 1877–1881, https://doi.org/10.1021/jacs.8b12827.
[33] M.J. Frisch, G.W. Trucks, H.B. Schlegel, G.E. Scuseria, M.A. Robb, J.R. Cheeseman, G. Scalmani, et al., Gaussian 16, Revision C.01, 2016, Gaussian, Inc., (Wallingford), 2025.
[34] Winmostar, Winmostar V10, X-Ability co. Ltd., Tokyo, Japan, 2019.
[35] B. Badger, B. Brocklehurst, Formation of dimer cations of aromatic hydrocarbons, Nature (London) 219 (1968) 263, https://doi.org/10.1038/219263a0.
[36] B. Badger, B. Brocklehurst, Absorption Spectra of Dimer Cations. Part 2—Benzene Derivatives, Trans. Faraday Soc. 65 (1969) 2582–2587, https://doi.org/10.1039/TF9696502582.
[37] C. Hansch, A. Leo, R.W.A. Taft, Survey of Hammett Substituent Constants and Resonance and Field Parameters, Chem. Rev. 91 (2) (1991) 165–195, https://doi.org/10.1021/cr00002a004.
[38] T. Papp, L. Kollár, T. Kégl, Employment of Quantum Chemical Descriptors for Hammett Constants: Revision Suggested for the Acetoxy Substituent, Chem. Phys. Lett. 588 (2013) 51–56, https://doi.org/10.1016/j.cplett.2013.10.017.
[39] S. Tojo, S. Toki, S. Takamuku, Formation and reactivity of dimer Radical cations of 4-Methoxystyrene, Radiat. Phys. Chem. 40 (2) (1992) 95–99, https://doi.org/10.1016/1359-0197(92)90064-M.
[40] M. Wojcik, M. Tachiya, Geminate charge recombination with distance-dependent intrinsic reaction rate: escape probability and its electric field effect, Radiat. Phys. Chem. 74 (3,4) (2005) 132–138, https://doi.org/10.1016/j.radphyschem.2005.04.005.
[41] Y. Wang, J.J. Tria, L.M. Dorfman, Identity and yield of positive charge Centers in irradiated Chloro hydrocarbon liquids and the rates of their interaction with solute molecules, J. Phys. Chem. 83 (15) (1979) 1944–1951, https://doi.org/10.1021/j100478a005.
[42] Y. Yamamoto, S. Nishida, K. Hayashi, Pulse Radiolysis Study of Salt Effects on Reactions of Aromatic Radical Cations with Cl^-. Rate Constants in the Absence and Presence of Quaternary Ammonium Salts, J. Chem. Soc. Faraday Trans. 1 83 (6) (1987) 1795–1804, https://doi.org/10.1039/F19878301795.
[43] D.Y. Yoon, P.R. Sundararajan, P.J. Flory, Conformational characteristics of polystyrene, Macromolecules 391 (19) (1974) 776–783, https://doi.org/10.1021/ma60048a019.
[44] S.E. Braslavsly, Glossary of Terms Used in Photochemistry 3rd Edition, Pure Appl. Chem. 79 (3) (2007) 293–465, https://doi.org/10.1351/pac200779030293.
[45] A.K. Croft, H.M. Howard-Jones, Chlorine–Benzene Cmplexes—the Reliability of Density Functionals for Non-Covalent Radical Complexes, Phys. Chem. Chem. Phys. 9 (2007) 5649–5655, https://doi.org/10.1039/B704966H.
[46] G.A. Russel, Solvent effects in the reactions of free radicals and atoms, 1957, J. Am. Chem. Soc. 79 (11) (1957) 2977–2978, https://doi.org/10.1021/ja01568a085.
[47] R.E. Bühler, M. Ebert, Transient charge-transfer complexes with chlorine atoms by pulse Radiolysis of carbon tetrachloride solutions, Nature 214 (1967) 1220–1221, https://doi.org/10.1038/2141220a0.
[48] A. Nakano, T. Kozawa, K. Okamoto, S. Tagawa, T. Kai, T. Shimokawa, Acid Generation Mechanism of Poly(4-Hydroxystyrene)-Based Chemically Amplified Resists For Post-Optical Lithography: Acid Yield and Deprotonation Behavior of Poly(4-Hydroxystyrene) and Poly(4-Methoxystyrene), Jpn. J. Appl. Phys. 245 (2006) 6866, https://doi.org/10.1143/JJAP.45.6866.
[49] K. Okamoto, S. Seki, S. Tagawa, Formation of trimer and dimer Radical cations of methyl-substituted benzenes in γ-irradiated low-temperature matrices, J. Phys. Chem. A 110 (26) (2006) 8073–8080, https://doi.org/10.1021/jp061527m.
[50] K. Okamoto, Y. Muroya, T. Kozawa, Dynamics of ionized poly(4-hydroxystyrene)-type Resist polymers with *tert*-Butoxycarbonyl-protecting group, Sci. Rep. 14 (2024) 16729, https://doi.org/10.1038/s41598-024-67794-0.